ORIGINAL PAPER

Seismic Bearing Capacity of Shallow Strip Footings on Sand Deposits with Weak Inter-layer

Hamed Haghsheno · Reza Jamshidi Chenari ⬤ · Sina Javankhoshdel · Tooraj Banirostam

Abstract The main objective of this study is to evaluate the ultimate seismic bearing capacity of a shallow strip footing resting on a frictional soil stratum containing a weak intervening layer. The majority of the studies throughout the literature pertain to the static loading condition. The previous seismic analyses have also been devoted to the studies on the bearing capacity of shallow strip footings resting on a two-layered soil. The influence of weak middle layer on the pseudo-static seismic bearing capacity of shallow foundations is the main focus of the present study. To determine the seismic bearing capacity, the limit equilibrium method (LEM) was combined with the pseudo-static seismic loading approach. Bearing capacity was defined by a single equivalent coefficient which combines the contributions of cohesion, surcharge and soil weight. A two-wedge failure surface, known as the Coulomb failure mechanism, was adopted to model the slip lines in each layer to calculate the seismic bearing capacity of the overlying shallow strip footing. The Particle Swarm Optimization (PSO) algorithm was invoked to seek the optimal bearing capacity value under different strength and loading conditions. In order to verify the validity of the presented formulations, the results were compared with some Finite Elements Method (FEM) analyses available in literature. Furthermore, the influence of the embedment depth, thickness, and strength of the weak inter-layer on the seismic bearing capacity of the shallow footing is investigated in the presence of different seismic loading arrangements. The results of this study could be very helpful in the seismic analysis and design of shallow foundations overlying a soil medium containing a weak layer of various strengths.

H. Haghsheno · R. Jamshidi Chenari (✉)
Department of Civil Engineering, Faculty of Engineering, University of Guilan, Rasht, Iran
e-mail: jamshidi_reza@yahoo.com;
jamshidi_reza@guilan.ac.ir

S. Javankhoshdel
Rocscience Inc., 54 Saint Patrick St, Toronto, ON, Canada

T. Banirostam
Central Tehran Branch, Islamic Azad University, Tehran, Iran

1 Introduction

Natural soils are often formed in discrete layers, and shallow foundations are sometimes located on soils with layered structures. Many researchers have investigated the problem of the bearing capacity of foundations resting on layered soils. The first approach employed to solve the bearing capacity of a foundation lain over a two-layer clay deposit under static loading

was presented by Button ([1953]). He assumed a general shear failure mechanism along with cylindrical slip surfaces emanating from the footing edges. Brown and Meyerhof ([1969]) investigated the ultimate bearing capacity of foundations resting on clay subsoils in the case of a stiff layer overlying a soft layer and vice versa. Their studies were based on model tests using circular and strip footings, making use of a range of layer thicknesses and clay strengths. Moreover, their analyses were carried out in terms of total stress. Concerning the stiff layers overlying the soft layers, they found that the dominant failure mechanism was the punching of the top layer, and the bearing capacity of shallow footings was based mainly on the shear resistance of the bottom layer. In the case of the soft layer overlying the stiff clay, failure occurred mainly by the soft layer being squeezed between the footing and the stiffer layer under the earth, with certain interactions among the layers as the strength ratio approached unity. Meyerhof ([1974]) studied the ultimate bearing capacity of footings resting on two-layer subsoils in the form of a dense sand layer over a soft clay layer and a loose sand layer over a layer of stiff clay. Different modes of the soil failure were analyzed and compared with those of model tests on circular and strip footings. Meyerhof and Hanna ([1978]) considered the case of a footing resting on a strong layer underlain by a weak deposit. In their failure mechanism, it was assumed that if the top layer was relatively thin, the failure would take place by the top layer being punched through, and the bottom layer undergoing a general shear failure. However, if the top layer was relatively thick, the failure mechanism would fully take place in the top clay layer. Florkiewicz ([1989]) presented a kinematically admissible plane-strain failure mechanism for a typical two-layer system and made use of the upper bound method to make estimations of the bearing capacity of the layered soils. He further compared the ultimate bearing capacity of strip footings obtained from the proposed approach with the experimental data available in literature and suggested that the method could be used for practical purposes. Michalowski and Shi ([1995]) presented a limit analysis approach (upper bound) to solve the bearing capacity of strip footings underlain by two-layer soil deposits. Their method was applicable to any combinations of the parameters of the two layers, yet the results could be only applied to the scenario of a layer of granular soils resting on clays.

They observed that the depth of the collapse mechanism was strongly dependent on the strength of the clay, such that very weak clays would attract the mechanism even at greater depths. Burd and Frydman ([1997]) carried out a study on the bearing capacity of sand layers overlying clay soils for the case where the thickness of the sand layer was comparable to the width of the rigid foundation placed over the soil surface. They further conducted a parametric study through both finite element and finite difference methods. The study was based on the use of the soil parameters obtained from an assessment of a range of possible values that might be expected to be relevant for full-scale structures. Their results illustrated that the shear strength of the clay had an important influence on the mechanisms of load spread within the fill. Merifield et al. ([1999]) employed a numerical technique to calculate both the lower and upper bounds of limit loads based on the static and kinematic theorems of limit analysis in order to determine the ultimate bearing capacity of surface strip footings resting on a horizontally-layered clay profile. They proposed a modified bearing capacity factor (N_c^*) as a function of H/B, where H was the thickness of the top layer and B was the footing width, and the strength ratio was equal to c_{u_1}/c_{u_2}, where c_{u1} and c_{u2} were the undrained shear strengths of the upper and lower clay layers, respectively. Wang and Carter ([2002]) conducted large deformation analyses, simulating the penetration of strip and circular footings into two-layered clays in which the upper layer was assumed stronger than the lower. The importance of large deformation analysis was illustrated by comparing the small and large deformation predictions. They evaluated the undrained bearing capacity factors for various cases involving different layer thicknesses and ratios of the undrained shear strengths of the two clay layers. They further illustrated the development of the plastic zones and the influence of the soil self-weight on the bearing capacity. Michalowski ([2002]) obtained upper-bound solutions for various degrees of load inclinations applied on foundations resting on two-layered clays while assuming two different failure mechanisms including a continually deforming field and a rigid-block mechanism separated by velocity discontinuity surfaces. He found that the rigid-block mechanism was able to produce better (lower) upper bounds compared to the continuously deforming field mechanism. This observation arises due to the fact that

the former is more flexible in assuming different geometries of the collapse mechanism. Merifield and Nguyen (2006) used the finite element analysis to predict the undrained bearing capacity of strip, square and circular footings resting on two-layered clay deposits with different layer thicknesses and soil properties. Moreover, they compared their results with previous solutions for strip footings on layered clays. Ghazavi and Eghbali (2008) employed the simple Coulomb failure mechanism and adapted it to a two-layered soil. They concluded that the results obtained from the finite element analysis matched very well with those obtained from the Coulomb failure mechanism, particularly when the difference between the shear strength parameters of the layers was low. Bandini and Pham (2011) studied the influence of embedment depth on the ultimate bearing capacity of strip footings on two-layered clays with relatively different shear strength parameters, using the finite element method. They presented the finite element results in terms of a modified bearing capacity factor that accounted for the footing embedment, relative shear strength and thickness of the two clay layers. Ahmadi and Mofarraj Kouchaki (2016) analyzed the bearing capacity of shallow strip footings resting on two-layered soils, revealing that general shear failure usually occurs in the case of weak-over-strong layer arrangement, while concerning strong-over-weak clay layered scheme, the soil would most likely experience punching failure with a large amount of plastic settlement prior to reaching its ultimate bearing capacity. They presented simple equations for both strong-over-weak and weak-over-strong arrangements.

Valore et al. (2017) conducted several experimental tests to evaluate the effect of the weak layer on the failure mechanisms and ultimate bearing capacity. The test results showed that the weak layer strongly influences both the ultimate bearing capacity and the failure mechanism provided that its depth is less than about four times the footing width. Moreover, they realized that a thin weak layer can lead to the decrease in the ultimate bearing capacity by up to 80%.

The majority of the studies reviewed through the literature pertain to the static loading condition. Very limited number of research studies is found, focused on the seismic bearing capacity of shallow foundations rested on layered deposits. Debnath and Ghosh (2018) used the limit equilibrium method based on the pseudo-static analysis to predict the bearing capacity of shallow

strip footings resting on two-layered soils. In their study the failure mechanism was assumed as linearly varying with depth with different wedge angles at each layer. The bearing capacity of a shallow strip footing in two-layered soils was presented as a single coefficient for the combined resistances of unit weight, surcharge, and cohesion. The authors showed that by increasing the strength parameters of the upper layer (such as γ, c, and φ), while those of the bottom layer remained constant, the seismic bearing capacity increased, or vice versa.

It is noted that the research of Debnath and Ghosh (2018) was based on the same assumptions of Ghosh and Debnath (2017), Jamshidi Chenari et al. (2018), Izadi et al. (2019a), Pakdel et al. (2019) and Izadi et al. (2019b) which were investigated for the determination of the seismic bearing capacity of single-layer soil.

The main objective of the present research is to evaluate the ultimate seismic bearing capacity of shallow strip footings resting on a three-layer soil deposit in form of a parent frictional material containing a weak inter-layer. The ultimate bearing capacity of the shallow strip footing was evaluated by the use of the limit equilibrium method combined with the pseudo-static approach. The particle swarm optimization (PSO) algorithm is used for the optimization, and the bearing capacity factor is presented in the form of an equivalent coefficient, $N_{\gamma(eq)}$. The results are first validated against some idealized assumptions available in the literature. Consequently, by considering the weak inter-layer contribution, its influence on the seismic bearing capacity of the overlying shallow footing will be investigated.

2 Model Definition

A strip footing with width B was assumed to lie on top of a weak inter-layered frictional soil deposit as shown in Fig. 1. The overburden pressure was idealized as a surcharge $q = \gamma D_f$. The bearing capacity of the strip footing, q_{ult} is normally computed using the following basic formulation:

$$q_{ult} = \frac{1}{2}\gamma B N_{\gamma_{(eq)}} \tag{1}$$

where $N_{\gamma_{(eq)}}$ is the equivalent single bearing capacity coefficient for the joint considerations of the unit weight, surcharge, and cohesion contributors, and γ is the unit weight of the parent sand deposit. It should be
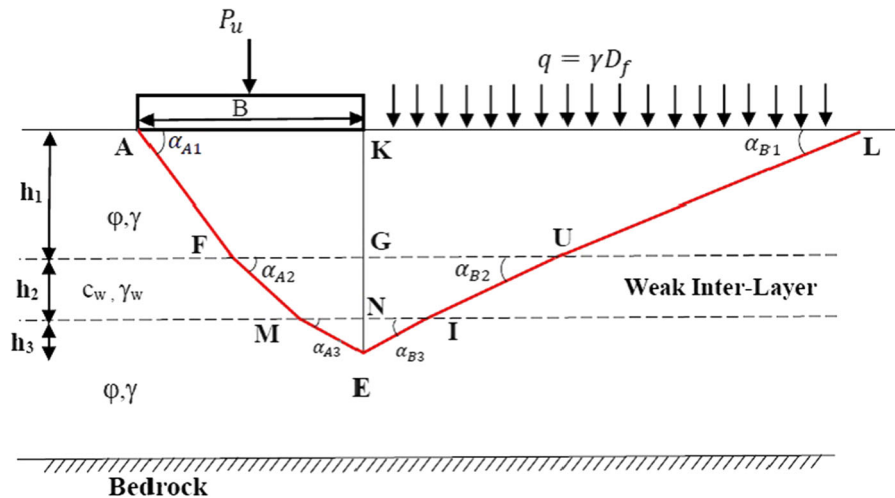
Fig. 1 Failure mechanism assumed in the present analysis

noted that in case the underlying sand deposit is intervened by a thin weak clay inter-layer, the equivalent unit weight does not undergo noticeable changes. Therefore, the parent unit weight can be employed instead.

Superimposed on Fig. 1 is a schematic diagram of the adopted failure mechanism with the original two-wedge slip surface proposed by Richards et al. (1993). As shown in Fig. 1, the vertical surface KGNE is assumed to behave like a virtual retaining wall on which, at the failure stage, active pressure resulting jointly from q_{ult}, as a surcharge, and the weight of the wedge KGNEMFA as the backfill soil, is applied from the left side. On the right-hand side, surcharge $q = \gamma D_f$ and the weight of the wedge KGNEIUL apply lateral passive pressure on the virtual wall. To satisfy equilibrium, the active and passive thrusts acting on the virtual wall must be equal.

3 Analysis Procedure

The assumptions made into the analytical procedure are: (i) weight of the soil above the base of the foundation was accounted for by assuming a uniform surcharge, (ii) the parent soil is frictional, homogeneous and isotropic, and (iii) the failure mechanism consists of the active and passive wedges with their inclinations sought as the optimization parameters in the present analyses. To determine the equivalent bearing capacity coefficient, $N_{\gamma_{(eq)}}$, the failure

mechanism of the problem has been depicted in Fig. 2 in dismantled wedges. In this figure, α_{Ai} and α_{Bi} are the slip surface angles at the ith layer in the active and passive zones, respectively, δ_i is the interface friction angle along the surface between the active and passive zones at the ith layer level, k_v is the vertical seismic acceleration coefficient, and k_h is the horizontal seismic acceleration coefficient.

The total active and passive resistances can be determined via Eqs. (2) and (3), respectively. Furthermore, it should be noted that the approximate 2:1 load distribution assumption has been adopted to estimate the total applied load/stress on the interface between the different failure wedges as illustrated in Fig. 2.

$$P_a = P_{a1} + P_{a2} + P_{a3} \tag{2}$$
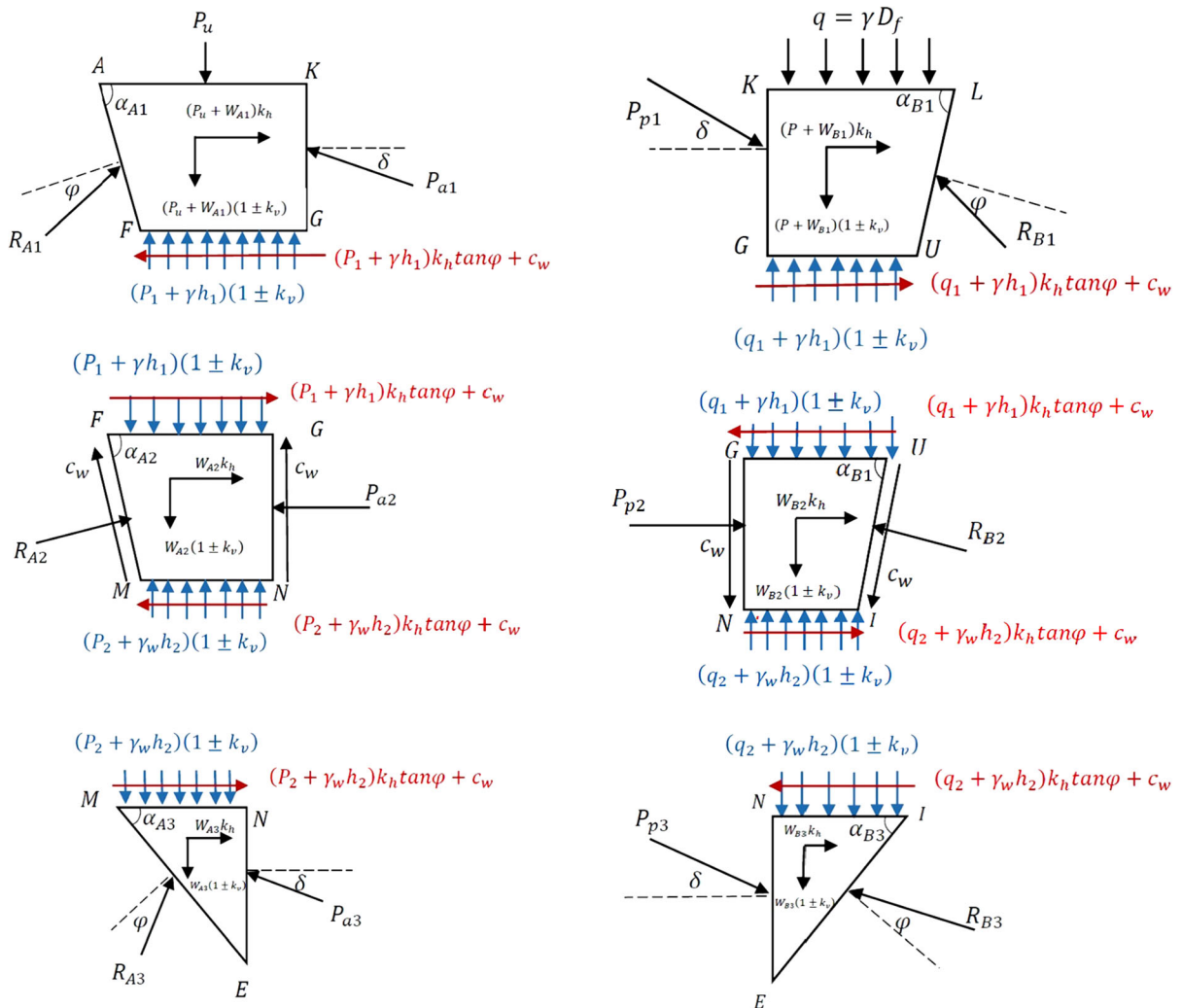
$$P_p = P_{p1} + P_{p2} + P_{p3} \tag{3}$$

Given the equilibrium of the wedges at three different levels, the active and passive forces are equated. Therefore, by equating the active pressure and passive resistance, the ultimate bearing capacity (q_{ult}), can be found:

$$P_a = P_p \tag{4}$$

$$q_{ult} = \frac{1}{2}\gamma B N_{\gamma_{(eq)}} \tag{5}$$

Therefore, $N_{\gamma_{(eq)}}$ becomes:

$$N_{\gamma_{(eq)}} = \frac{b}{a} + \frac{d}{a} + \left(\frac{2c_w}{\gamma B}\right)\frac{e}{a} \tag{6}$$

Fig. 2 Free body diagrams of the active and passive wedges

Detailed equations for a, b, d and e are given in the "Appendix".

Particle swarm optimization (PSO), which is a population-based stochastic optimization technique, inspired by the social behavior of flocking birds, was invoked to come up with the optimum solution in different parameters sets. MATLAB Mathworks was employed for this purpose.

4 Validation of the Proposed Formulations

To verify the accuracy of the presented limit equilibrium formulations, the findings were validated against the solutions presented by Debnath and Ghosh (2018), for foundations resting on a two-layer deposit. To this end, the three-layer arrangement was reduced to a simple two-layer case for comparison purpose only. It was further endorsed by comparing the current findings against those of Ghazavi and Eghbali (2008) conducted through both LEM and Finite Elements (FE) analyses using PLAXIS. To this end, two different sets of the internal friction angle and unit weight were adopted for the two layers, whereas the top layer thickness was varied to yield the thickness ratio h_1/B ranging from 0 to 1. Constant overburden pressure values of 17.5kN/m^2 and 25kN/m^2 were applied for the footing widths of 2 m and 3 m, respectively. Table 1 shows the results of validation

analyses in comparison to the similar results found in the literature. Generally, good agreement is found between the current results and the literature. However, the current formulation renders bearing capacity estimations closer to Debnath and Ghosh (2018). This very good agreement lies at the similarity of the calculation formulations in between the two studies.

5 Parametric Study

In order to assess the influence of the weak inter-layer on $N_{\gamma(eq)}$, the soil profile was considered as shown in Fig. 1. For this purpose, the weak inter-layer was assumed a thin intervening layer with trivial cohesion and thickness values as specified in Table 2.

Static and seismic bearing capacity of the shallow footing over the weak inter-layered deposit have been illustrated in Figs. 3 and 4, respectively. Two observations were made through comparison of different parts of the bearing capacity charts in Figs. 3 and 4. The thickness of the weak inter-layer contributes more importantly to the bearing capacity of shallow footings over sand deposits. It was seen that decreasing the thickness of the weak clay-type inter-layer will give rise to less reduction in the bearing capacity of the overlying footings. In addition, the position of the weak inter-layer affects the degree to which $N_{\gamma(eq)}$ reduces. At limit where the weak inter-layer acts as a

**Table 2** Design soil properties for weak-layer arrangement deposit

Parameter	Values
$\frac{h_1}{B}$	0.1–1.0
$\frac{h_2}{B}$	0.001, 0.01, 0.02, 0.05, 0.1, 0.2
$\frac{2q}{\gamma B}$	0.5
φ (°)	25, 30, 35
$\frac{\delta}{\varphi}$	0.5
$\frac{2c_w}{\gamma B}$	0.25, 0.5, 1, 2
$\frac{\gamma_w}{\gamma}$	0.8
k_h	0, 0.05, 0.10, 0.015, 0.20, 0.25 0.30
k_v/k_h	0, 0.5, 1

very thin lens, it is observed that there is a critical embedment depth at which its adverse influence on the bearing capacity of the overlying shallow footing becomes most highlighted. $\frac{h_2}{B} = 0.5$ is seemingly considered as the critical embedment depth of the weak inter-layer, corresponding to the minimum bearing capacity of the shallow footing as appears from different parts of Fig. 3.

As far as the seismic bearing capacity of the shallow footing underlain by a weak inter-layered deposit is concerned, it is obvious from Fig. 4 that the critical embedment position of the weak layer become

**Table 1** Bearing capacity estimations obtained from the present formulations compared with the literature

| q_{ult} (kN/m^2)										
B(m)	h1/B	h1	$\varphi_1 = 34°$ and $\varphi_2 = 37°$				$\varphi_1 = 39°$ and $\varphi_2 = 42°$			
			Ghazavi and Eghbali (2008)		Debnath and Ghosh (2018)	Present study	Ghazavi and Eghbali (2008)		Debnath and Ghosh (2018)	Present study
			LEM	FEM (PLAXIS)	LEM	LEM	LEM	FEM (PLAXIS)	LEM	LEM
2	0.25	0.5	1649	1740	1639	1680.27	3824	3719	3804	3779.594
	0.5	1	1569	1510	1430	1467.98	3652	3235	3132	3294.17
	0.75	1.5	1482	1389	1379	1323.29	3463	2959	2938	2953.37
	1	2	1390	1165	1331	1251.48	3258	2693	2861	2756.69
3	0.25	0.75	2435	2561	2986	2469.55	5657	5238	7004	5565.508
	0.5	1.5	2317	2222	2784	2156.34	5404	4858	5867	4848.56
	0.75	2.25	2189	1899	2651	1943.49	5125	4341	5695	4346.82
	1	3	2053	1731	2630	1839.18	4820	3906	5408	4054.22
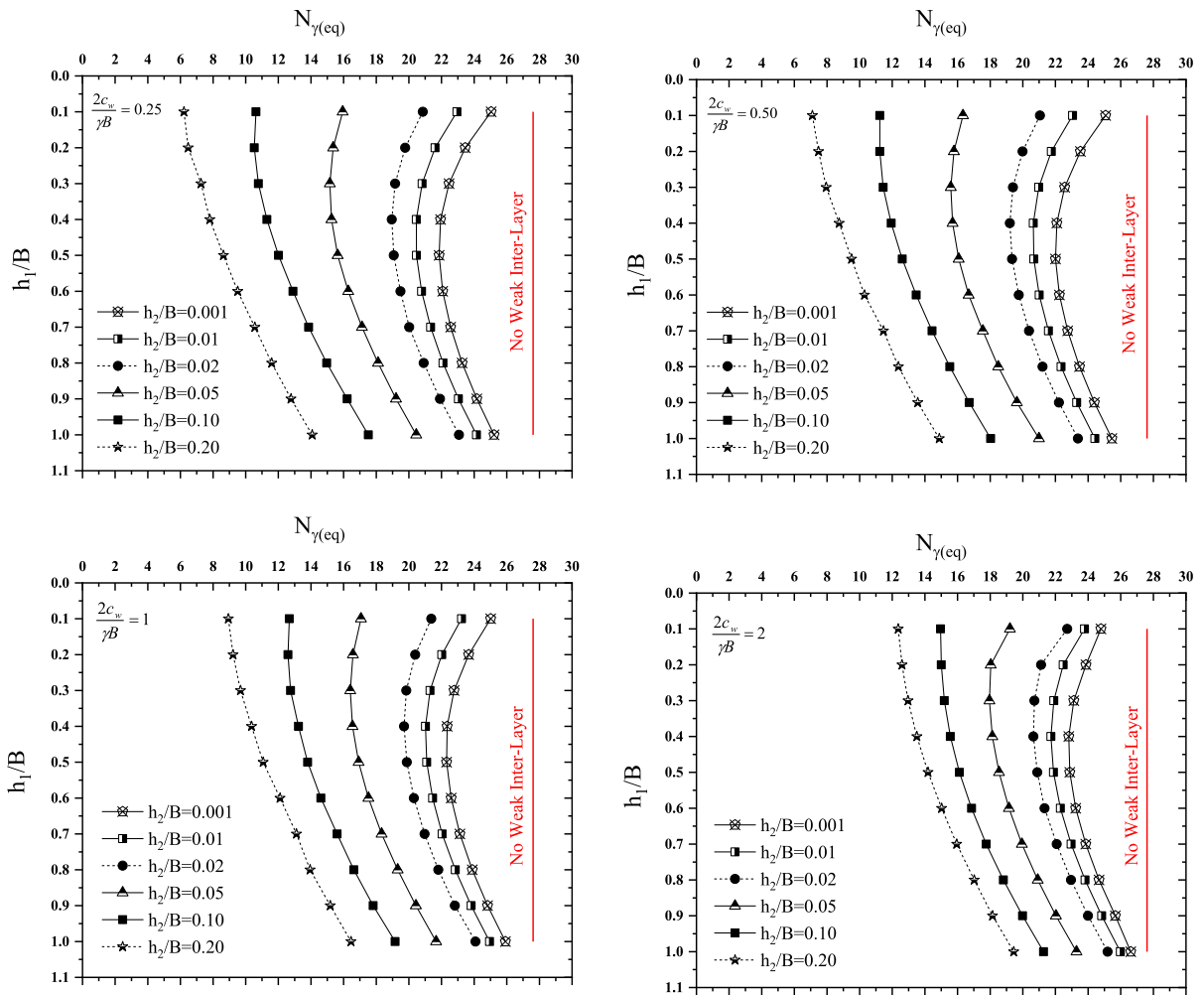
Fig. 3 Influence of the weak inter-layer embedment position and thickness on the static bearing capacity of shallow footings, $\varphi = 30°, \frac{2c_w}{\gamma B} = 0.25, 0.5, 1, 2$

shallower. This lends support to the contention that the horizontally directed seismic loading moves the shear failure mechanism of the overlying shallow footing upward as addressed by Izadi et al. (2019a). Another observation from Fig. 4 is that the horizontal earthquake acceleration coefficient brings about more reduction in the bearing capacity of the shallow footing, albeit in a distorted-shape profile of variation with depth. The vertical earthquake acceleration coefficient, on the other hand, did not show any prominent influence on the bearing capacity of shallow footings rested on a weak inter-layered frictional deposit as it affects both the motive and resistor forces, at least for frictional materials.

The trend of variation of $N_{\gamma(eq)}$ with h_1/B presented in Figs. 3 and 4, can be explained with the aid of Fig. 5 in which Z is the depth of the failure wedge and is equal to $0.5B \times \tan(45 + 0.5\varphi)$. P_a and P_p are the active and passive pressures, respectively. Moreover, d is the point of force application for the passive and active pressures and equals $0.58B$ based on the specifications of the problem chosen for Figs. 3 and 4 and the equation determining the failure wedge depth (Bowles 1996). In static condition, the weak clay inter-layer with a low cohesion value gives rise to a reduction in the depth of the failure wedge (Z). Therefore, the value of d presumably becomes lower than $0.58B$. Regarding the aforementioned depth and
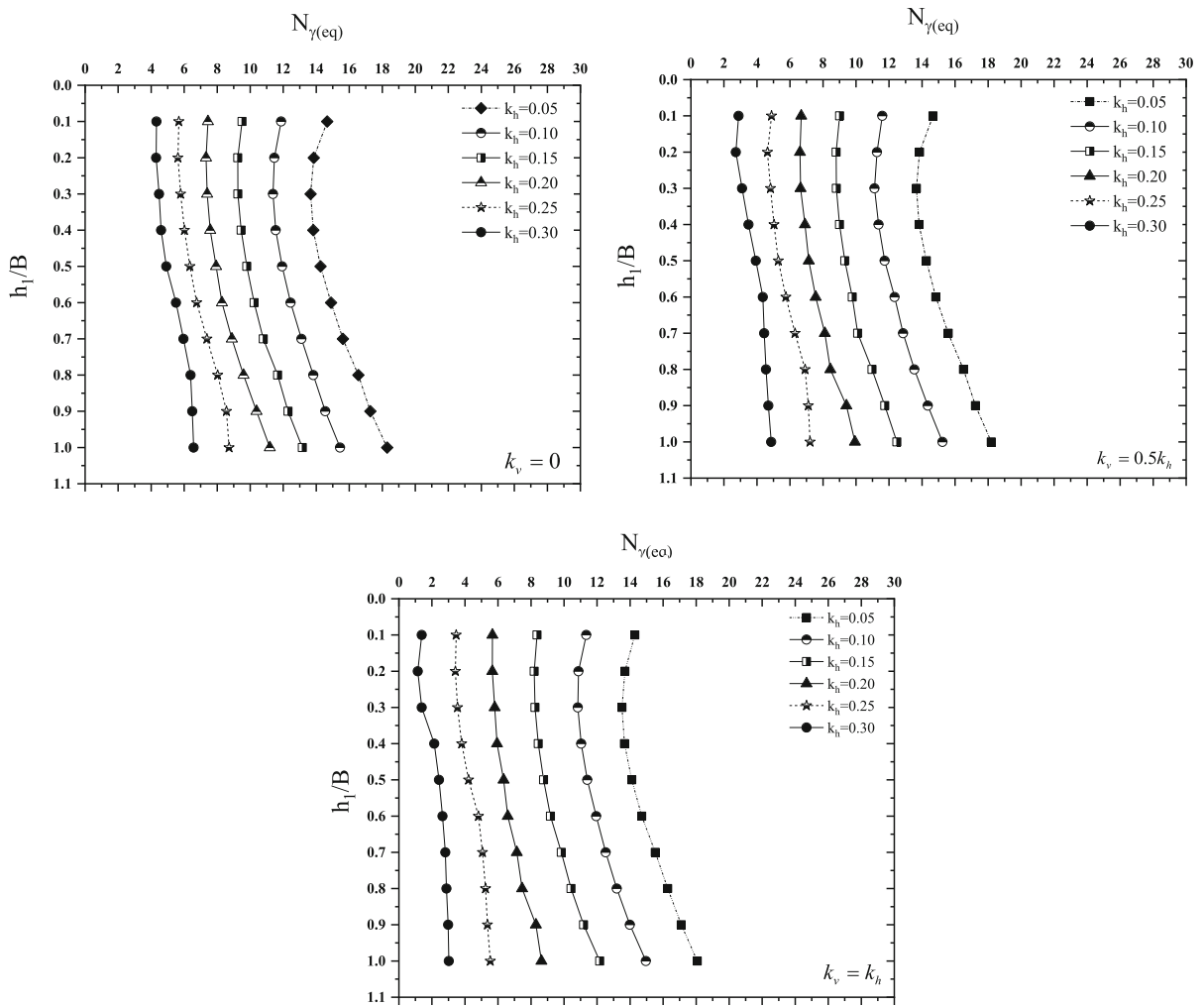
Fig. 4 Seismic bearing capacity of shallow foundations rested on frictional deposits with weak clay inter-layer, $\varphi = 30°, \frac{h_2}{B} = 0.01, \frac{2c_w}{\gamma B} = 0.25$
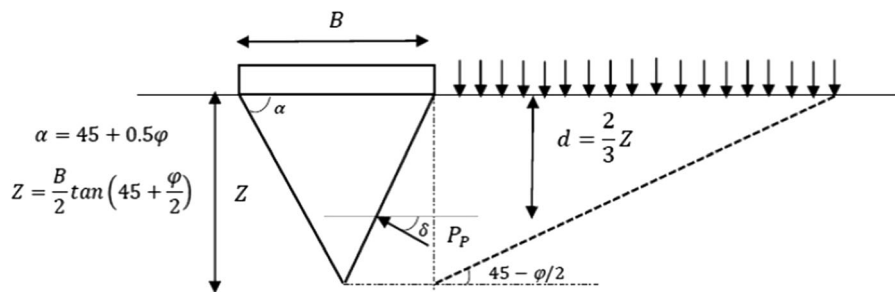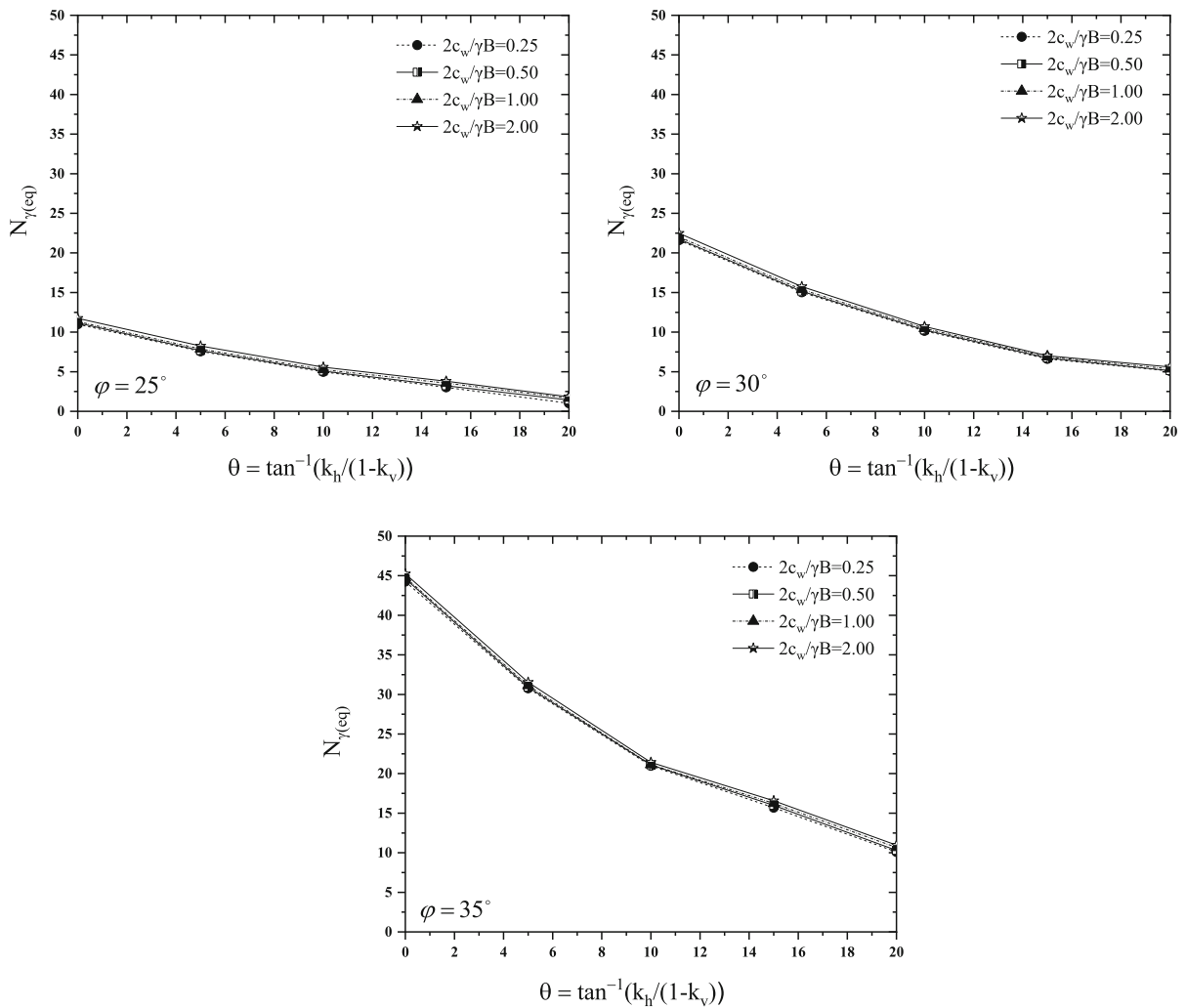

Fig. 5 Point of the active/passive force application (Bowles 1996)

the point of force application, d is considered as the critical depth of the weak inter-layer. The existence of a weak inter-layer at the approximate depth of 0.5B has therefore the greatest influence on the reduction of the $N_{\gamma(eq)}$ value as shown in the different parts of Fig. 3.
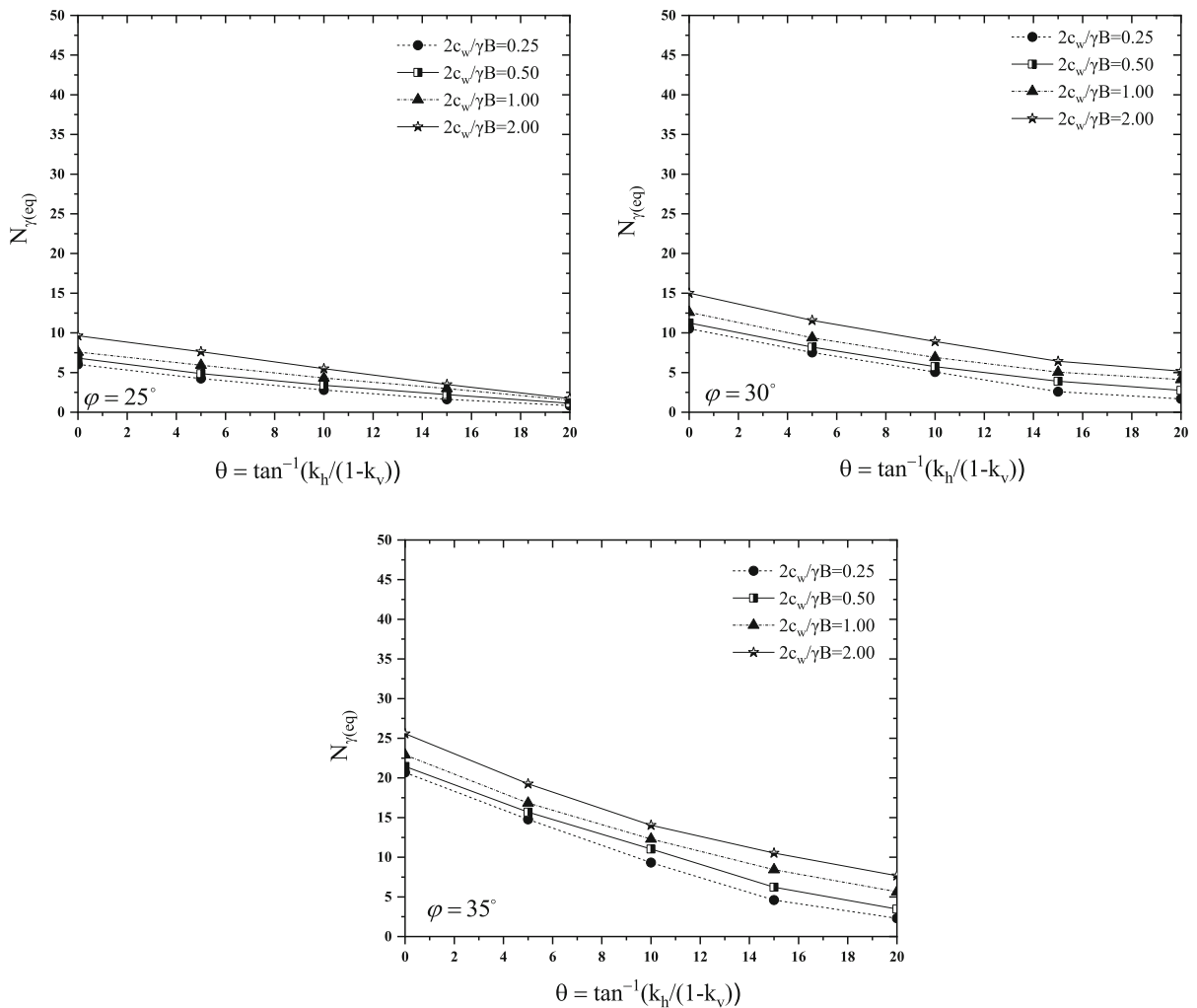
Fig. 6 Influence of the earthquake coefficients on the bearing capacity of shallow footings rested on frictional deposits with weak clay inter-layer, $\frac{h_1}{B} = 0.2 \,\&\, \frac{h_2}{B} = 0.01$

In seismic loading conditions, the value of the friction angle (φ) is reduced (Das and Ramana 2011). As a result of this reduction in φ, the depth of the failure wedge and the point of force application is diminished as well. Therefore, the depth of the point of force application has been found to be shallower than the corresponding value obtained in the static loading condition. For this reason, the value of $N_{\gamma(eq)}$ decreases with the increase in h_1/B up to 0.4 for $k_h \leq 0.20$ as depicted in Fig. 4, yet when h_1/B is greater than 0.4, the value of $N_{\gamma(eq)}$ increases, hence, the critical depth of the weak inter-layer is around 0.4B.

A similar trend of behavior is observed for the values of k_h which are higher than 0.2. The critical

depth of embedment for the weak clay inter-layer, however, reduces to 0.2B. This is due to the reduction of the depth of the failure wedge and the point of force application accordingly. Izadi et al. (2019a) clearly indicated that the pseudo-static loading condition brings about formation of the shallower failure mechanism which in effect endorses the findings of the current research.

The joint contribution of the horizontal and vertical earthquake acceleration coefficients has been reflected in a single parameter, namely the seismic angle defined as $\theta = tan^{-1}\left(\frac{k_h}{1-k_v}\right)$. This parameter represents the angle of deviation of the gravitational forces from

Fig. 7 Influence of the earthquake coefficients on the bearing capacity of shallow footings rested on frictional deposits with weak clay inter-layer, $\frac{h_1}{B} = 0.2 \& \frac{h_2}{B} = 0.1$

the plumb line position due to the earthquake load application. Figures 6 and 7 show the influence of the vertical and horizontal seismic acceleration coefficients, reflected in a lumped parameter, on the value of $N_\gamma(eq)$. Two different weak inter-layer geometric conditions have been considered and each figure contains information on three different internal friction angles and also various weak inter-layer cohesion values. For all conditions, it is evident that the value of $N_\gamma(eq)$ decreases with the increase in the value of θ as expected. However, it is noted that in seismic loading condition the bearing capacity of the overlying shallow foundation is less influenced by the shear strength parameters of the weak inter-layer when it is

in lens size. To be more specific, for pseudo-static loading condition, when the weak inter-layer becomes thicker, its cohesion will be playing more eminent role as appears from Fig. 7. In other words, for seismic loading condition, decremented cohesion value of the weak inter-layer embedded at critical depth, will yield substantial reduction in the bearing capacity of the overlying footing.

6 Conclusions

In the present study, an effort was made to evaluate the equivalent bearing capacity coefficient of shallow

strip footings resting on a sand deposit intervened by a weak inter-layer, through the use of the limit equilibrium method and a pseudo-static loading approach. The LEM formulations were implemented into a MATLAB code and the PSO algorithm was employed for the optimization process. The thickness and embedment depth of the weak cohesive inter-layer was sought for both static and seismic loading conditions. To this end, the horizontal and vertical earthquake acceleration coefficients were considered and integrated into a single seismic angle. Followings are the main findings of the current research:

1. Formation of a weak intervention in soil deposits will bring about some degrees of reduction in bearing capacity of overlying shallow foundations, depending on the thickness and embedment depth of the weak inter-layer.

2. For both static and seismic loading conditions, there is always an optimum embedment depth of the weak inter-layer. For the static loading scheme, it was found that the critical embedment depth is nearly 0.5B. However, the critical embedment depth displaces upward for pseudo-static loading condition. This is attributed to the shallower failure mechanism due to horizontal seismic loading. In case of seismic loading, it was shown that the critical embedment depth diminishes to 0.2B.

3. The weak inter-layer thickness was shown to impart an augmented reduction in the bearing capacity of the overlying shallow foundation. Furthermore, it was proved that at critical embedment depth, the level of bearing capacity loss for different inter-layer thicknesses and strength parameters of the parent medium always remains higher that 20%.

4. It was indicated that a very thin weak inter-layer of 0.001B thick suffices to bring about notable reduction in the bearing capacity of the shallow footings rested atop.

5. It was deduced that the cohesion value of the intervening weak layer emerges to be more influential when the weak inter-layer thickness is more tangible.

6. Seismic loading condition gives rise to substantial decrease in the bearing capacity of the shallow footing rested on a frictional soil deposit intervened by a weak clay inter-layer. However, this reduction was found to be more importantly attributed to the horizontal earthquake acceleration application as the vertical acceleration component bears a dual stability impact. To be more specific, it reduces both the motive and resistor forces.

7. Pseudo-static acceleration coefficients, lumped into the seismic angle parameter was shown to have some threshold values depending on the internal friction angle of the host medium. It is evident that the internal friction angle of the parent soil deposit can be considered as an upper bound to the applied seismic angle.

Appendix: Analytical Functions of

Eq. (6)

$$\begin{aligned}
a = & \left[\frac{(1-k_h)\sin(\alpha_{A1}-\varphi) + k_h\cos(\alpha_{A1}-\varphi)}{\cos(\alpha_{A1}-\varphi-\delta)} \right] - \frac{\left(1 - \frac{h_1}{B}\cot\alpha_{A1}\right)}{\left(1 + \frac{h_1}{B}\right)} \left[\frac{(1-k_v)\sin(\alpha_{A1}-\varphi) + k_h\cos(\alpha_{A1}-\varphi)tan\varphi}{\cos(\alpha_{A1}-\varphi-\delta)} \right] \\
& + \frac{\left(1 - \frac{h_1}{B}\cot\alpha_{A1}\right)}{\left(1 + \frac{h_1}{B}\right)} \left[\frac{(1-k_v)\sin(\alpha_{A2}) + k_h\cos(\alpha_{A2})tan\varphi}{\cos(\alpha_{A2})} \right] \\
& - \frac{\left(1 - \frac{h_1}{B}\cot\alpha_{A1}\right)\left(1 - \frac{h_1}{B}\cot\alpha_{A1} - \frac{h_2}{B}\cot\alpha_{A2}\right)}{\left(1 + \frac{h_1}{B}\right)\left(1 - \frac{h_1}{B}\cot\alpha_{A1} + \frac{h_2}{B}\right)} \left[\frac{(1-k_v)\sin(\alpha_{A2}) + k_h\cos(\alpha_{A2})tan\varphi}{\cos(\alpha_{A2})} \right] \\
& + \frac{\left(1 - \frac{h_1}{B}\cot\alpha_{A1}\right)\left(1 - \frac{h_1}{B}\cot\alpha_{A1} - \frac{h_2}{B}\cot\alpha_{A2}\right)}{\left(1 + \frac{h_1}{B}\right)\left(1 - \frac{h_1}{B}\cot\alpha_{A1} + \frac{h_2}{B}\right)} \left[\frac{(1-k_v)\sin(\alpha_{A3}-\varphi) + k_h\cos(\alpha_{A3}-\varphi)tan\varphi}{\cos(\alpha_{A3}-\varphi-\delta)} \right]
\end{aligned}$$

$$d = 2\frac{D_f}{B}\left(\frac{h_3}{B}\cot\alpha_{B3} + \frac{h_2}{B}\cot\alpha_{B2} + \frac{h_1}{B}\cot\alpha_{B1}\right)\left[\frac{(1-k_v)\sin(\alpha_{B1}+\varphi) - k_h\cos(\alpha_{B1}+\varphi)}{\cos(\alpha_{B1}+\varphi+\delta)}\right]$$

$$-\frac{2\frac{D_f}{B}\left(\frac{h_3}{B}\cot\alpha_{B3}+\frac{h_2}{B}\cot\alpha_{B2}+\frac{h_1}{B}\cot\alpha_{B1}\right)\left(\frac{h_3}{B}\cot\alpha_{B3}+\frac{h_2}{B}\cot\alpha_{B2}\right)}{\frac{h_3}{B}\cot\alpha_{B3}+\frac{h_2}{B}\cot\alpha_{B2}+\frac{h_1}{B}\cot\alpha_{B1}+\frac{h_1}{B}}\left[\frac{(1-k_v)\sin(\alpha_{B1}+\varphi)}{\cos(\alpha_{B1}+\varphi+\delta)}+\frac{k_h\cos(\alpha_{B1}+\varphi)tan\varphi}{\cos(\alpha_{B1}+\varphi+\delta)}\right]$$

$$+\frac{2\frac{D_f}{B}\left(\frac{h_3}{B}\cot\alpha_{B3}+\frac{h_2}{B}\cot\alpha_{B2}+\frac{h_1}{B}\cot\alpha_{B1}\right)\left(\frac{h_3}{B}\cot\alpha_{B3}+\frac{h_2}{B}\cot\alpha_{B2}\right)}{\left(\frac{h_3}{B}\cot\alpha_{B3}+\frac{h_2}{B}\cot\alpha_{B2}+\frac{h_1}{B}\cot\alpha_{B1}+\frac{h_1}{B}\right)}\left[\frac{(1-k_v)\sin\alpha_{B2}+k_h\cos\alpha_{B2}tan\varphi}{\cos\alpha_{B2}}\right]$$

$$-\frac{2\frac{D_f}{B}\left(\frac{h_3}{B}\cot\alpha_{B3}+\frac{h_2}{B}\cot\alpha_{B2}+\frac{h_1}{B}\cot\alpha_{B1}\right)\left(\frac{h_3}{B}\cot\alpha_{B3}+\frac{h_2}{B}\cot\alpha_{B2}\right)\left(\frac{h_3}{B}\cot\alpha_{B3}\right)}{\left(\frac{h_3}{B}\cot\alpha_{B3}+\frac{h_2}{B}\cot\alpha_{B2}+\frac{h_1}{B}\cot\alpha_{B1}+\frac{h_1}{B}\right)\left(\frac{h_3}{B}\cot\alpha_{B3}+\frac{h_2}{B}\cot\alpha_{B2}+\frac{h_2}{B}\right)}\left[\frac{(1-k_v)\sin\alpha_{B2}+k_h\cos\alpha_{B2}}{\cos\alpha_{B2}}\right]$$

$$+\frac{2\frac{D_f}{B}\left(\frac{h_3}{B}\cot\alpha_{B3}+h_2\cot\alpha_{B2}+\frac{h_1}{B}\cot\alpha_{B1}\right)\left(\frac{h_3}{B}\cot\alpha_{B3}+\frac{h_2}{B}\cot\alpha_{B2}\right)\left(\frac{h_3}{B}\cot\alpha_{B3}\right)}{\left(\frac{h_3}{B}\cot\alpha_{B3}+\frac{h_2}{B}\cot\alpha_{B2}+\frac{h_1}{B}\cot\alpha_{B1}+\frac{h_1}{B}\right)\left(\frac{h_3}{B}\cot\alpha_{B3}+\frac{h_2}{B}\cot\alpha_{B2}+\frac{h_2}{B}\right)}\left[\frac{(1-k_v)\sin(\alpha_{B3}+\varphi)+k_h\cos(\alpha_{B3}+\varphi)tan\varphi}{\cos(\alpha_{B3}+\varphi+\delta)}\right]$$

$$e = 2\frac{h_2}{B}\tan\alpha_{A2} + 2\frac{h_2}{B}\tan\alpha_{B2} + 2\frac{h_2}{B}cot\alpha_{B2} + \frac{\left(1-\frac{h_1}{B}\cot\alpha_{A1}\right)\cos(\alpha_{A1}-\varphi)}{\cos(\alpha_{A1}-\varphi-\delta)}$$

$$-\frac{\left(\frac{h_3}{B}\cot\alpha_{B3}+\frac{h_2}{B}\cot\alpha_{B2}-\frac{h_1}{B}cot\alpha_{B1}\right)\cos(\alpha_{B1}+\varphi)}{\cos(\alpha_{B1}+\varphi+\delta)} - \frac{\left(1-\frac{h_1}{B}\cot\alpha_{A1}-\frac{h_2}{B}\cot\alpha_{A2}\right)\cos(\alpha_{A3}-\varphi)}{\cos(\alpha_{A3}-\varphi-\delta)}$$

$$+\frac{\left(\frac{h_3}{B}\cot\alpha_{B3}\right)\cos(\alpha_{B3}+\varphi)}{\cos(\alpha_{B3}+\varphi+\delta)}$$

$$
\begin{aligned}
b =\; & 2\frac{h_1}{B}\left(\frac{h_3}{B}\cot\alpha_{B3} + \frac{h_2}{B}\cot\alpha_{B2} + 0.5\frac{h_1}{B}\cot\alpha_{B1}\right)\left[\frac{(1-k_h)\sin(\alpha_{B1}+\varphi) - k_h\cos(\alpha_{B1}+\varphi)}{\cos(\alpha_{B1}+\varphi+\delta)}\right] \\
& - 2\frac{h_1}{B}\left(\frac{h_3}{B}\cot\alpha_{B3} + \frac{h_2}{B}\cot\alpha_{B2}\right)\left[\frac{(1-k_v)\sin(\alpha_{B1}+\varphi_1) + k_h\cos(\alpha_{B1}+\varphi)\tan\varphi}{\cos(\alpha_{B1}+\varphi+\delta)}\right] \\
& - \frac{2\frac{h_1}{B}\frac{h_3}{B}\cot\alpha_{B3}\left(\frac{h_3}{B}\cot\alpha_{B3} + \frac{h_2}{B}\cot\alpha_{B2}\right)}{\left(\frac{h_3}{B}\cot\alpha_{B3} + \frac{h_2}{B}\cot\alpha_{B2} + \frac{h_2}{B}\right)}\left[\frac{(1-k_v)\sin\alpha_{B2} + k_h\cos\alpha_{B2}}{\cos\alpha_{B2}}\right] \\
& + 2\frac{h_1}{B}\left(\frac{h_3}{B}\cot\alpha_{B3} + \frac{h_2}{B}\cot\alpha_{B2}\right)\left[\frac{(1-k_v)\sin\alpha_{B2} + k_h\cos\alpha_{B2}\tan\varphi}{\cos\alpha_{B2}}\right] \\
& + 2\frac{\gamma_w}{\gamma}\frac{h_2}{B}\left(\frac{h_3}{B}\cot\alpha_{B3} + 0.5\frac{h_2}{B}\cot\alpha_{B2}\right)\left[\frac{(1-k_v)\sin\alpha_{B2} - k_h\cos\alpha_{B2}}{\cos\alpha_{B2}}\right] \\
& - 2\frac{\gamma_w}{\gamma}\frac{h_2}{B}\frac{h_3}{B}\cot\alpha_{B3}\left[\frac{(1-k_v)\sin\alpha_{B2} + k_h\cos\alpha_{B2}}{\cos\alpha_{B2}}\right] \\
& + \frac{2\frac{h_1}{B}\frac{h_3}{B}\cot\alpha_{B3}\left(\frac{h_3}{B}\cot\alpha_{B3} + \frac{h_2}{B}\cot\alpha_{B2}\right)}{\left(\frac{h_3}{B}\cot\alpha_{B3} + \frac{h_2}{B}\cot\alpha_{B2} + \frac{h_2}{B}\right)}\left[\frac{(1-k_v)\sin(\alpha_{B3}+\varphi) + k_h\cos(\alpha_{B3}+\varphi)\tan\varphi}{\cos(\alpha_{B3}+\varphi+\delta)}\right] \\
& + 2\frac{\gamma_w}{\gamma}\frac{h_2}{B}\frac{h_3}{B}\cot\alpha_{B3}\left[\frac{(1-k_v)\sin(\alpha_{B3}+\varphi) + k_h\cos(\alpha_{B3}+\varphi)\tan\varphi}{\cos(\alpha_{B3}+\varphi+\delta)}\right] \\
& + \frac{2\frac{h_1}{B}\left(1 - \frac{h_1}{B}\cot\alpha_{A1}\right)\left(1 - \frac{h_1}{B}\cot\alpha_{A1} - \frac{h_2}{B}\cot\alpha_{A2}\right)}{\left(1 - \frac{h_1}{B}\cot\alpha_{A1}\right) + \frac{h_2}{B}}\left[\frac{(1-k_v)\sin\alpha_{A2} + k_h\cos\alpha_{A2}\tan\varphi}{\cos\alpha_{A2}}\right] \\
& - \frac{2\frac{h_1}{B}\left(1 - \frac{h_1}{B}\cot\alpha_{A1} - \frac{h_2}{B}\cot\alpha_{A2}\right)}{\left(1 - \frac{h_1}{B}\cot\alpha_{A1}\right) + \frac{h_2}{B}}\left[\frac{(1-k_v)\sin(\alpha_{A3}-\varphi) + k_h\cos(\alpha_{A3}-\varphi)\tan\varphi}{\cos(\alpha_{A3}-\varphi-\delta)}\right] \\
& + 2\frac{h_1}{B}\left(1 - \frac{h_1}{B}\cot\alpha_{A1}\right)\left[\frac{(1-k_v)\sin(\alpha_{A1}-\varphi) + k_h\cos(\alpha_{A1}-\varphi)\tan\varphi}{\cos(\alpha_{A1}-\varphi-\delta)}\right] \\
& - 2\frac{h_1}{B}\left(1 - 0.5\frac{h_1}{B}\cot\alpha_{A1}\right)\left[\frac{(1-k_v)\sin(\alpha_{A1}-\varphi) + k_h\cos(\alpha_{A1}-\varphi)}{\cos(\alpha_{A1}-\varphi-\delta)}\right] \\
& - 2\frac{h_1}{B}\left(1 - \frac{h_1}{B}\cot\alpha_{A1}\right)\left[\frac{(1-K_v)\sin\alpha_{A2} + K_h\cos\alpha_{A2}\tan\varphi_{ave}}{\cos\alpha_{A2}}\right] \\
& + 2\frac{\gamma_w}{\gamma}\frac{h_2}{B}\left(1 - \frac{h_1}{B}\cot\alpha_{A1} - \frac{h_2}{B}\cot\alpha_{A2}\right)\left[\frac{(1-k_v)\sin\alpha_{A2} + k_h\cos\alpha_{A2}\tan\varphi}{\cos\alpha_{A2}}\right] \\
& - 2\frac{\gamma_w}{\bar{\gamma}}\frac{h_2}{B}\left(1 - \frac{h_1}{B}\cot\alpha_{A1} - 0.5\frac{h_2}{B}\cot\alpha_{A2}\right)\left[\frac{(1-k_v)\sin\alpha_{A2} + k_h\cos\alpha_{A2}}{\cos\alpha_{A2}}\right] \\
& - 2\frac{\gamma_w}{\gamma}\frac{h_2}{B}\left(1 - \frac{h_1}{B}\cot\alpha_{A1} - \frac{h_2}{B}\cot\alpha_{A2}\right)\left[\frac{(1-k_v)\sin(\alpha_{A3}-\varphi) + k_h\cos(\alpha_{A3}-\varphi)\tan\varphi}{\cos(\alpha_{A3}-\varphi-\delta)}\right] \\
& + \left(\frac{h_3}{B}\right)^2\cot\alpha_{B3}\left[\frac{(1-k_v)\sin(\alpha_{B3}+\varphi) - k_h\cos(\alpha_{B3}+\varphi)}{\cos(\alpha_{B3}+\varphi+\delta)}\right] \\
& - \frac{h_3}{B}\left(1 - \frac{h_1}{B}\cot\alpha_{A1} - \frac{h_2}{B}\cot\alpha_{A2}\right)\left[\frac{(1-k_v)\sin(\alpha_{A3}-\varphi) + k_h\cos(\alpha_{A3}-\varphi)}{\cos(\alpha_{A3}-\varphi-\delta)}\right]
\end{aligned}
$$

References

Ahmadi M, Mofarraj Kouchaki B (2016) New and simple equations for ultimate bearing capacity of strip footings on two-layered clays: numerical study. Int J Geomech 16(4):06015014

Bandini P, Pham H (2011) Bearing capacity of embedded strip footings in two-layered clay soils Reston, VA: ASCEProceedings of the Geo-Frontiers 2011 conference, March 13–16, 2011, Dallas, Texas|d 20110000: American Society of Civil Engineers.

Brown J, Meyerhof G (1969) Experimental study of bearing capacity in layered clays. In: Soil Mech & Fdn Eng Conf Proc/Mexico/

Bowles L (1996) Foundation analysis and design. McGraw-hill, New York

Burd H, Frydman S (1997) Bearing capacity of plane-strain footings on layered soils. Can Geotech J 34(2):241–253

Button SJ (1953) The bearing capacity of footings on a two-layer cohesive subsoil. In: Proc. 3rd Int. Conf. Soil Mech. Found. Engng, Zurich , vol 1, pp 332–335.

Das B, Ramana G (2011) Principles of Soil Dynamics, Second. International SI édition, Cengage Learning, USA

Debnath L, Ghosh S (2018) Pseudostatic analysis of shallow strip footing resting on two-layered soil. Int J Geomech 18(3):04017161

Florkiewicz A (1989) Upper bound to bearing capacity of layered soils. Can Geotech J 26(4):730–736

Ghazavi M, Eghbali AH (2008) A simple limit equilibrium approach for calculation of ultimate bearing capacity of shallow foundations on two-layered granular soils. Geotech Geol Eng 26(5):535–542

Ghosh S, Debnath L (2017) Seismic bearing capacity of shallow strip footing with coulomb failure mechanism using limit equilibrium method. Geotech Geol Eng 35(6):2647–2661

Jamshidi Chenari R, Izadi A, Nazemi Sabet Somehsaraei M (2018) Discussion of "seismic Bearing Capacity of Shallow Strip Footing with Coulomb Failure Mechanism Using Limit Equilibrium Method" by S. Ghosh, L. Debnath. December 2017, Volume 35, Issue 6, Pp. 2647–2661. Geotech Geol Eng 36(6):4037–4040

Izadi A, Nazemi Sabet Soumehsaraei M, Jamshidi Chenari R, Ghorbani A (2019a) Pseudo-static bearing capacity of shallow foundations on heterogeneous marine deposits using limit equilibrium method. Mar Georesour Geotechnol 37(10):1163–1174

Izadi A, Nazemi Sabet Soumehsaraei M, Jamshidi Chenari R, Moallemi S, Javankhoshdel S (2019b) Spectral bearing capacity analysis of strip footings under pseudo-dynamic excitation. Geomech Geoengin. https://doi.org/10.1080/17486025.2019.1670873

Merifield R, Nguyen V (2006) Two-and three-dimensional bearing-capacity solutions for footings on two-layered clays. Geomech Geoeng Int J 1(2):151–162

Merifield R, Sloan S, Yu H (1999) Rigorous plasticity solutions for the bearing capacity of two-layered clays. Geotechnique 49(4):471–490

Meyerhof G (1974) Ultimate bearing capacity of footings on sand layer overlying clay. Can Geotech J 11(2):223–229

Meyerhof G, Hanna A (1978) Ultimate bearing capacity of foundations on layered soils under inclined load. Can Geotech J 15(4):565–572

Michalowski RL (2002) Collapse loads over two-layer clay foundation soils. Soils Found 42(1):1–7

Michalowski RL, Shi L (1995) Bearing capacity of footings over two-layer foundation soils. J Geotech Eng 121(5):421–428

Pakdel P, Jamshidi Chenari R, Veiskarami M (2019) Seismic bearing capacity of shallow foundations rested on anisotropic deposits. Int J Geotech Eng. https://doi.org/10.1080/19386362.2019.1655983

Richards R Jr, Elms D, Budhu M (1993) Seismic bearing capacity and settlements of foundations. J Geotech Eng 119(4):662–674

Valore C, Ziccarelli M, Muscolino SR (2017) The bearing capacity of footings on sand with a weak layer. Geotech Res 4(1):12–29

Wang C, Carter J (2002) Deep penetration of strip and circular footings into layered clays. Int J Geomech 2(2):205–232